$$-\frac{l\pi}{c}\frac{n\pi}{a}\sin\frac{n\pi x}{a}\cos\frac{n\pi x'}{a}\sin\frac{m\pi y}{b}\sin\frac{m\pi y'}{b}\cos\frac{l\pi z}{c}\sin\frac{l\pi z'}{c}\hat{x}\hat{x}$$

$$-\frac{n\pi}{a}\frac{l\pi}{c}\cos\frac{n\pi x}{a}\sin\frac{n\pi x'}{a}\sin\frac{m\pi y}{b}\sin\frac{m\pi y'}{b}\sin\frac{l\pi z}{c}\cos\frac{l\pi z'}{c}\hat{z}\hat{z}\Bigg\}. \quad (28)$$

The main difference between (27) and (20) is the appearance of the terms $-(\delta(r-r')/k^2)\mathbf{I}$ and $(\delta(r-r')/k^2)\hat{z}\hat{z}$ in them, respectively. This indicates that if the current source is transverse in the waveguide, we will not obtain any term like $-(1/j\omega\epsilon)J_z(r)\hat{z}$ in the computation of the $E$ field, whereas the components $-(1/j\omega\epsilon)\cdot[J_x(r)\hat{x}+J_y(r)\hat{y}]$ will show up in the computation of the $E$ field in the cavity. The aforementioned difference between the equations results because we used the functional exp $(-\Gamma_{nm}\mid z-z'\mid)$ for the waveguide case. This function has special characteristics when one computes its derivatives [(15) and (18)]. In other words, the infinite nature of the waveguide comes into the picture when one computes $\mathbf{G}_e$ for the waveguide.

## IV. CONCLUSION

It is possible to construct the complete dyadic Green's function by employing the scalar eigenfunction of the Helmholtz equation. Care must be exercised in defining the derivatives in the sense of distribution and in using the correct completeness relation in order to compute the correct dyadic Green's function. This leads to the computation of the $E$ field in the entire structure as well. The procedure discussed in this short paper may also be used to determine the complete form of the dyadic Green's function for nonrectangular waveguides and cavities.

## ACKNOWLEDGMENT

The author wishes to thank Prof. R. Mittra, Dr. T. Itoh, and W. Pearson for helpful discussions.

## REFERENCES

[1] R. E. Collin, "On the incompleteness of $E$ and $H$ modes in wave guides," *Can. J. Phys.*, vol. 51, pp. 1135–1140, 1973.
[2] C. T. Tai, "On the eigen-function expansion of dyadic Green's functions," Univ. Michigan, Ann Arbor, Tech. Rep., Apr. 1973.
[3] ——, *Dyadic Green's Functions in Electromagnetic Theory*. Scranton, Pa.: Educational Pubs., 1971.
[4] G. Goubau, *Electromagnetic Waveguides and Cavities*. New York: Pergamon, 1961, pp. 88–237.
[5] J. Arsac, *Fourier Transforms and the Theory of Distribution*. Englewood Cliffs, N. J.: Prentice-Hall, 1966.
[6] A. H. Zemanian, *Distribution Theory and Transform Analysis*. New York: McGraw-Hill, 1965.

# Enhancement of Surface-Acoustic-Wave Piezoelectric Coupling in Three-Layer Substrates

A. VENEMA AND J. J. M. DEKKERS

***Abstract*—Numerical results with respect to the piezoelectric coupling of a three-layer substrate (CdS–$SiO_2$–Si) are presented. ⟨111⟩-cut Si is used, and the direction of propagation is [11$\bar{2}$], the $SiO_2$ layer is amorphous and the CdS layer (hexagonal, 6 mm) has the $c$ axis normal to the substrate. The choice of these materials is connected with the integration of acoustic surface-wave devices on silicon. The interesting result is that, depending on the applied transducer configuration for particular values of $kh$ of the $SiO_2$ and CdS layer, an increase in the piezoelectric coupling occurs. Its maximum exceeds the value of the coupling in the two-layer substrates: CdS–$SiO_2$ and CdS–Si, therefore more effective interdigital transducers can be designed for three-layer substrates.**

Manuscript received December 24, 1974; revised March 31, 1975.

A. Venema is with the Department of Electrical Engineering, Delft University of Technology, Delft, The Netherlands.
J. J. M. Dekkers was with the Department of Electrical Engineering, Delft University of Technology, Delft, The Netherlands. He is now with the Institut für Halbleitertechnik, Rheinisch-Westfälische Technische Hochschule, Aachen, Germany.

The integration of frequency-selective acoustic surface-wave devices on silicon (Si) substrates has interesting device aspects [1]. Of particular interest are the structures which can be combined with p-n circuits and which can be realized by the application of silicon planar technology to one monolithic device. Since silicon is nonpiezoelectric, thin-film piezoelectric areas, including interdigital transducers, are necessary to convert electrical signal energy into acoustical energy. Cadmium sulfide (CdS) and zinc oxide (ZnO) are two materials commonly used in the construction of piezoelectric films.

To be compatible with silicon planar technology, the piezoelectric film must be separated from the silicon substrate by a (thermally grown) silicon dioxide ($SiO_2$) layer. This layer also provides an electrical insulation between the silicon substrate and the interdigital transducer, in case the configurations $A$ or $B$ are used (Fig. 1). In our calculations, however, the electrical conductivity of the silicon is assumed to be zero. This then leads to a substrate consisting of three layers, with Si and $SiO_2$ as essential materials. The ⟨111⟩-cut silicon wafer has a scribing flat in the ⟨11$\bar{2}$⟩ plane.

An important design parameter for surface-wave interdigital transducers is the piezoelectric coupling coefficient $K$ that is a measure of electrical to acoustical energy conversion and vice versa. $K$ has been calculated from the relative change $\Delta v/v$ in the phase velocity $v$, when an electrically perfect conducting plane is placed at the position of the interdigital transducer [2]; $K^2 = 2\mid \Delta v/v \mid$ (approximately). The present calculations are an application of the theory of elastic wave propagation in thin layers, as given by Farnell and Adler [3], to a three-layer substrate CdS–$SiO_2$–Si. This is in contrast to Armstrong and Crampin [4], and Fahmy and Adler [5], who used a matrix formulation to perform these calculations on multilayer substrates.

The following specifications and assumptions are made (Fig. 1).

The layers are considered to be free of any loss.

The CdS layer (hexagonal, 6mm) has the $c$ axis normal to the substrate surface.

The amorphous $SiO_2$ layer is considered electrically and elastically equivalent to fused quartz.

The Si substrate is ⟨111⟩ cut, coplanar with the $X_1$–$X_2$ plane and considered as a half-space.

The constants of the CdS and Si material were taken from Slobodnik and Conway [6] and those for used quartz were from Auld [7].

The mass loading due to the conducting planes is neglected.

The three-layer substrate is unbounded in the $X_1$–$X_2$ plane.

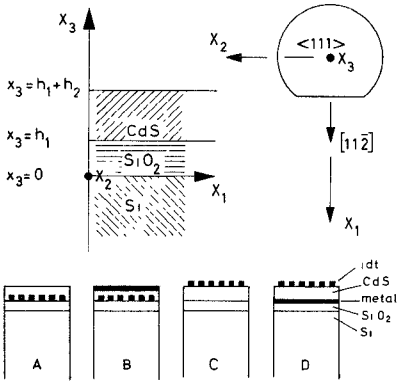


Fig. 1. Three-layer substrate with four possible transducer configurations.

The propagation direction $X_1$, for the surface wave, is collinear with $[11\bar{2}]$.

The surface waves are "straight-crested" waves, with wavenumber $k$. For this propagation direction the surface wave is polarized in the sagittal plane, i.e., components of the displacement and the electric field in the $X_2$ directions are zero.

Solie [8] found an enhancement in the piezoelectric coupling of two-layer substrates, i.e., when a piezoelectric substrate was overlaid by a nonpiezoelectric film, or a nonpiezoelectric substrate by a piezoelectric film. An even greater enhancement is found in the three-layer case considered here. The enhancement is defined relative to the CdS–$SiO_2$ substrate, because its piezoelectric coupling is generally higher than that in the CdS–Si case. The CdS–Si substrate is denoted by $kh_1 = 0$ and the CdS–$SiO_2$ substrate by $kh_1 = \infty$.

## RESULTS

*Configuration A (Fig. 2)*

Curve $kh_1 = 1$: the maximum enhancement is 23 percent ($kh_2 = 1.33$).

Curve $kh_1 = 0.5$: the maximum enhancement is 20 percent ($kh_2 = 1.33$).

Curve $kh_1 = 0.25$: the maximum enhancement is 10 percent ($kh_2 = 1.66$).

*Configuration B (Fig. 3).*

To avoid too weak signals $\Delta v/v$ must not be taken lower than, e.g., 0.001.

*First Peak*

Curve $kh_1 = 1$: the enhancement increases from zero ($kh_2 = 0$) to a maximum value of about 8 percent ($kh_2 = 0.42$).

Curve $kh_1 = 0.5$: the enhancement increases from 3 percent ($kh_2 = 0.33$), 25 percent ($kh_2 = 0.5$) to a maximum value of 38 percent ($kh_2 = 0.66$).

Curve $kh_1 = 0.25$: the enhancement increases from 14 percent ($kh_2 = 0.5$), 52 percent ($kh_2 = 0.66$) to high values.

Curve $kh_1 = 0.1$: the enhancement is about 15 percent ($kh_2 = 0.58$).

*Second Peak*

Curve $kh_1 = 1$: the enhancement decreases from 86 percent ($kh_2 = 1.33$), 57 percent ($kh_2 = 1.50$), 24 percent ($kh_2 = 2.00$), 12 percent ($kh_2 = 2.50$) to zero.

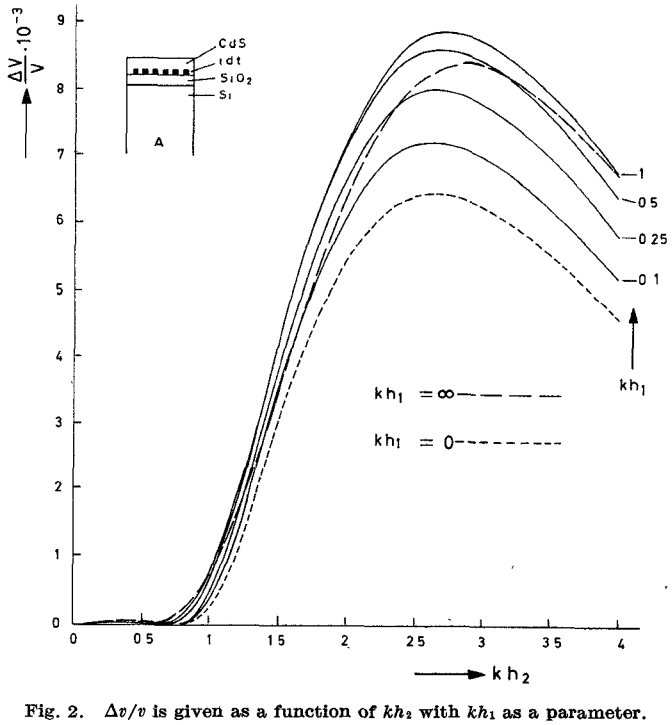


Fig. 2. $\Delta v/v$ is given as a function of $kh_2$ with $kh_1$ as a parameter.

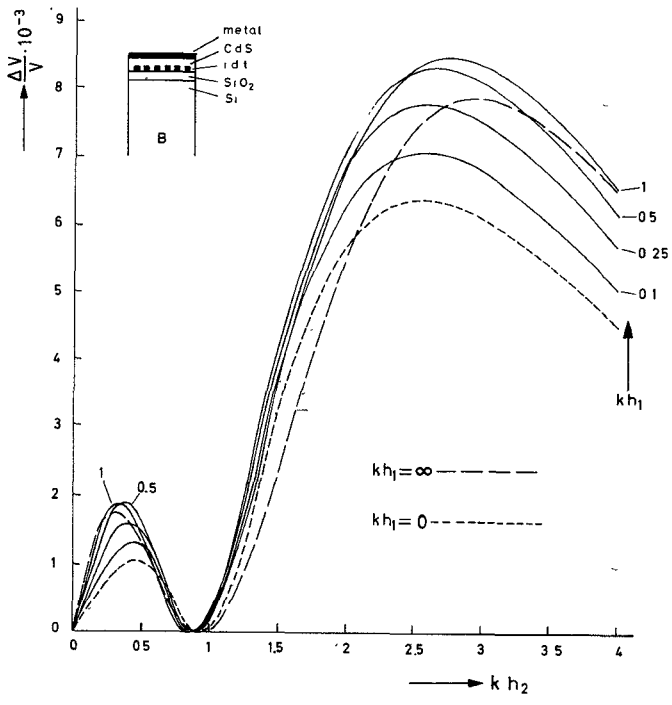


Fig. 3. $\Delta v/v$ is given as a function of $kh_2$ with $kh_1$ as a parameter.

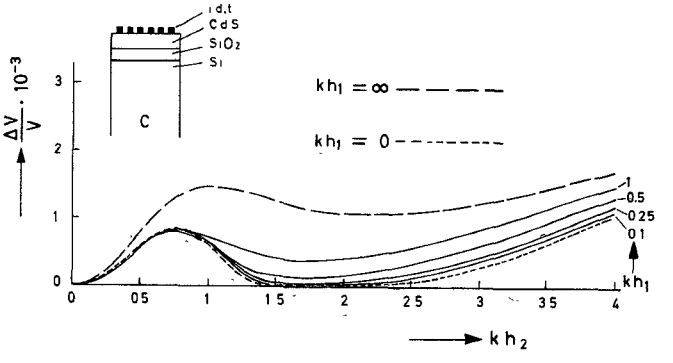


Fig. 4. $\Delta v/v$ is given as a function of $kh_2$ with $kh_1$ as a parameter.

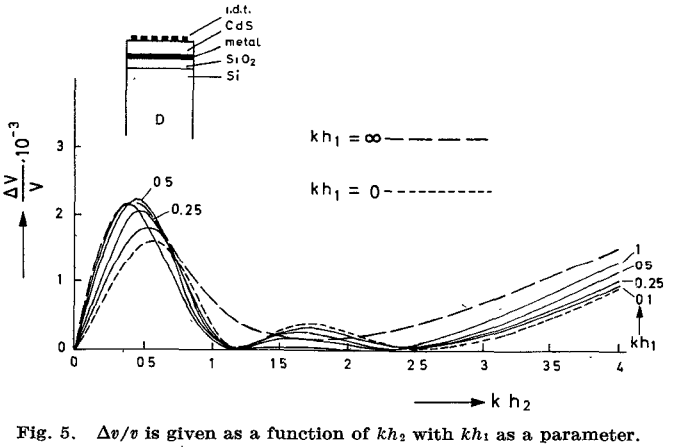


Fig. 5. $\Delta v/v$ is given as a function of $kh_2$ with $kh_1$ as a parameter.

Curve $kh_1 = 0.5$: the enhancement decreases from more than 100 percent ($kh_2 = 1.33$), 72 percent ($kh_2 = 1.50$), 28 percent ($kh_2 = 2.00$), 11 percent ($kh_2 = 2.50$) to zero.

Curve $kh_1 = 0.25$: the enhancement decreases from 92 percent ($kh_2 = 1.33$), 67 percent ($kh_2 = 1.50$), 24 percent ($kh_2 = 2.00$), 5 percent ($kh_2 = 2.50$) to zero.

Curve $kh_1 = 0.1$: the enhancement decreases from 70 percent

($kh_2 = 1.33$), 54 percent ($kh_2 = 1.50$), 14 percent ($kh_2 = 2.00$) to zero.

*Configuration C (Fig. 4)*

For this configuration no enhancement is found.

*Configuration D (Fig. 5)*

Curve $kh_1 = 0.5$: a small enhancement of about 2 percent is present in the range $kh_2 = 0.38$ to 0.5.


## ACKNOWLEDGMENT

The authors wish to thank Prof. S. Middelhoek and Dr. G. de Jong for valuable discussions.


## REFERENCES


[1] F. S. Hickernell, "The role of layered structures in surface acoustic wave technology," in *1973 Proc. IEEE Conf. Component Performance and Systems Applications of Surface Acoustic Wave Devices* (Aviemore, Scotland, 1973), pp. 11–21, Conf. Publ. 109.

[2] J. J. Campbell and W. R. Jones, "A method for estimating optimal crystal cuts and propagation directions for excitation of piezoelectric surface waves," *IEEE Trans. Sonics Ultrason.*, vol. SU-15, pp. 209–217, Oct. 1968.

[3] G. W. Farnell and E. L. Adler, "Elastic wave propagation in thin layers," in *Physical Acoustics*, vol. 9, W. P. Mason, Ed. New York: Academic, 1972.

[4] G. A. Armstrong and S. Crampin, "Piezoelectric surface wave calculations in multilayered anisotropic media," *Electron. Lett.*, vol. 8, pp. 521–522, 1972.

[5] A. H. Fahmy and E. L. Adler, "Propagation of acoustic surface waves in multilayers: A matrix description," *Appl. Phys. Lett.*, vol. 22, pp. 495–497, May 1973.

[6] A. J. Slobodnik and E. D. Conway, "Surface wave velocities," in *Microwave Acoustics Handbook*, USAF Res. Lab., Cambridge, Mass., Rep. AFCRL-70-0164, 1970.

[7] B. A. Auld, *Acoustic Fields and Waves in Solids*, vol. 1. New York: Wiley, 1973.

[8] L. P. Solie, "Piezoelectric wave on layered substrates," *J. Appl. Phys.*, vol. 44, pp. 619–627, Feb. 1973.


# Microwave Propagation in Rectangular Waveguide Containing a Semiconductor Subject to a Transverse Magnetic Field

J. B. NESS AND M. W. GUNN

*Abstract*—**The propagation constant of waveguide partially loaded with a semiconductor in the *H* plane is evaluated using a three-mode approximation analysis. As the waveguide is progressively filled, a large peak occurs in the attenuation coefficient due to higher order mode propagation. In the presence of a transverse magnetic field, propagation becomes nonreciprocal and this nonreciprocal effect is shown to be significantly increased in the region of the peak. The theoretical results are verified using n-type germanium samples in 26.5–40-GHz waveguide.**

## INTRODUCTION

The propagation characteristics of rectangular waveguide loaded with dielectric or semiconductor slabs have been investigated by many researchers [1]–[4], and these characteristics have been used to measure material properties or as a basis for construction of microwave devices. Semiconductor loading presents a more difficult problem for analysis than lossless dielectric, and if the semiconductor material is anisotropic, as occurs in the presence of a magnetic field, the problem is further complicated.

Waveguide partially loaded with a semiconductor subject to a transverse magnetic field may exhibit nonreciprocal propagation, and the possibility exists of constructing isolators, circulators, variable attenuators, etc., using semiconductor-loaded waveguide. Such nonreciprocal propagation has been studied experimentally [5], [6], and approximate theoretical analyses for both reciprocal and nonreciprocal propagation have been given by several authors [7]–[9]. Experimental devices such as isolators and power dividers have also been constructed [5], [10].

An approximation technique due to Schelkunoff [11] was used by Arnold and Rosenbaum [12] to analyze the partially loaded waveguide shown in Fig. 1. An approximate solution for the propagation constant was obtained using a two-mode ($TE_{10}$ and $TM_{11}$) analysis, and was shown to give reasonable agreement with experimental results.

In this short paper, a three-mode ($TE_{10}$, $TE_{11}$, $TM_{11}$) analysis is used, and although the mathematics becomes more complex, an improvement in accuracy is evident and certain aspects of the propagation constant are illustrated more clearly.

## THEORY

For a semiconductor subject to a transverse magnetic field, as shown in Fig. 1, the permittivity becomes a tensor given by [7], [12].

$$[\epsilon] = \begin{bmatrix} \epsilon_{11} & 0 & 0 \\ 0 & \epsilon_{22} & \epsilon_{23} \\ 0 & \epsilon_{32} & \epsilon_{33} \end{bmatrix}$$

$$\epsilon_{11} = \epsilon_0\epsilon_r\left[1 - \frac{j\sigma}{\omega\epsilon_0\epsilon_r}\right]$$

$$\epsilon_{22} = \epsilon_{33} = \epsilon_0\epsilon_r\left[1 - \frac{j\sigma}{\omega\epsilon_0\epsilon_r[1 + (R_cB_0\sigma)^2]}\right]$$

$$\epsilon_{23} = -\epsilon_{32} = \frac{jR_cB_0\sigma^2}{\omega[1 + (R_cB_0\sigma)^2]}$$

where

- $R_c$ Hall coefficient;
- $\sigma$ dc conductivity;
- $B_0$ magnetic-field strength;
- $\epsilon_r$ relative permittivity.

The simplifying assumptions that only one type of carrier is present and that the signal frequency $\omega$ is much less than the scattering frequency so that $\sigma$ is essentially constant, are used in the preceding equations. Thus the semiconductor parameters and the magnetic field enter the problem through the tensor permittivity.

For the two-mode approximation, the method of obtaining the propagation constant is given by Arnold and Rosenbaum [12] and the three-mode analysis is similar except that a sixth-order polynomial in $\gamma$, the propagation coefficient, is obtained, i.e.,

$$\gamma^6 + A_5\gamma^5 + A_4\gamma^4 + A_3\gamma^3 + A_2\gamma^2 + A_1\gamma + A_0 = 0 \qquad (1)$$

where all $A_n$ are in general complex. The analytical forms of the coefficients $A_0, \cdots, A_5$ are given in the Appendix.

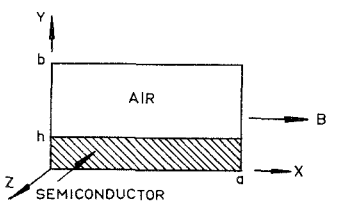


Fig. 1. Partially filled rectangular guide.

Manuscript received November 13, 1974; revised May 5, 1975. This work was supported in part by the Australian Research Grants Committee and the Australian Radio Research Board.

The authors are with the Department of Electrical Engineering, University of Queensland, Brisbane, Qld., Australia.